Flow instabilities due to the interfacial formation of surfactant–fatty acid material in a Hele-Shaw cell

Zahra Niroobakhsh, Matthew Litman, and Andrew Belmonte

Phys. Rev. E **96**, 053102 — Published 6 November 2017

DOI: 10.1103/PhysRevE.96.053102

Flow instabilities due to the interfacial formation of surfactant/fatty acid material in a Hele-Shaw cell

Zahra Niroobakhsh[†], Matthew Litman[‡], and Andrew Belmonte[†,‡*]
[†] *Dept of Materials Science & Engineering, Pennsylvania State University, University Park, PA 16802*
[‡] *Dept of Mathematics, Pennsylvania State University, University Park, PA 16802*
(Dated: June 23, 2017)

We present an experimental study of pattern formation during the penetration of an aqueous surfactant solution into a liquid fatty acid in a Hele-Shaw cell. When a solution of the cationic surfactant cetylpyridinium chloride is injected into oleic acid, a wide variety of fingering patterns are observed as a function of surfactant concentration and flow rate, which are strikingly different than the classic Saffman-Taylor (ST) instability. We observe evidence of interfacial material forming between the two liquids, causing these instabilities. Moreover, the number of fingers decreases with increasing flow rate Q, while the average finger width increases with Q, both trends opposite to the ST case. Bulk rheology on related mixtures indicates a gel-like state. Comparison of experiments using other oils indicates the importance of pH and the carboxylic headgroup in the formation of the surfactant/fatty acid material.

The Hele-Shaw experiment is a simple, classic system in fluid dynamics for studying quasi-2D instabilities and interface dynamics under reproducible and controlled conditions: two solid plates separated by a small gap filled with fluid. In their 1958 paper, Saffman & Taylor used a Hele-Shaw cell as a convenient surrogate for porous media flow, and showed that when another, less viscous fluid is injected into a more viscous one, fingers develop at the interface between the two fluids [1]. This well-known Saffman-Taylor (ST) instability was originally seen with Newtonian fluids [1, 2], however it has since been studied in more complex, non-Newtonian liquids such as polymer solutions [3–7], clay slurries [8, 9], foams [10], and colloidal suspensions [9].

When a reaction occurs at the interface between the two fluids in this system, new phenomena and other patterns distinct from the ST instability are also possible [11]. A rich variety of fingering patterns have been seen due to chemical reactions [12–14], precipitation reactions/chemical gardens [15–18], gel-producing reactions [19, 20], and micellar reactions [21]. This last case involves an interface between surfactant and organic ion solutions, which when well-mixed lead to wormlike micellar fluids [21, 22]. Precipitation reactions are also being used for CO_2 sequestration in Hele-Shaw cells [23].

Although oil and water are immiscible, certain oils are comprised of molecules which interact with aqueous solutions at an interface. For instance, precipitation and gel formation reactions are known to occur between crude oil (and its derivatives) and water [24–26]. Interfacial gel-like material has been observed in immiscible systems of aqueous cationic surfactants and oil-based fatty acids [20, 27, 28]. Unlike reactive interfaces in the wormlike micelle system [21, 22], these interfaces can pinch-off and form droplets, due to the additional presence of surface tension effects [27, 28]. Surface wrinkling is also seen in these systems, as well as crude oil derived asphaltenes at oil/water interfaces [26–28]. Here we focus on this general class of oils in contact with surfactant solutions injected in a Hele-Shaw cell, exploring the striking, finely textured patterns resulting from an interfacially forming material (see Fig. 1).

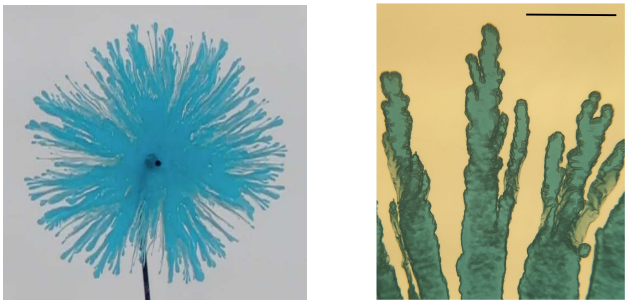

FIG. 1. (a) Instability pattern of a 400 mM CPCl solution injected into oleic acid at $Q = 100$ ml/h ($t = 10$ s); (b) close-up of the CPCl/oleic fingers taken about 10 min after finishing the test, showing clearly the material at the interface. Scale bar represents 5 mm.

The experiment consists of a Hele-Shaw cell, comprised of two $15{\times}15$ cm^2 glass plates separated by a gap $h = 100$ μm held fixed by brass shims at the corners, and initially filled with oil. We used various oils such as oleic acid (technical grade 90%, Alfa Aesar), caprylic acid (98%, Alfa Aesar), tetradecane (98%, TCI), and 1000 cS silicone oil (polydimethylsiloxane, BOSS Products). The experiments were done at room temperature, $21.5 - 23.5°$C. An aqueous solution of cetylpyridinium chloride (CPCl, Sigma Aldrich) at concentration C (0.5 to 425 mM) is injected between the plates through a hole at the center of the lower plate, at a fixed flow rate Q ranging from 5 to 400 ml/h. The solutions are made from purified, deionized water. A metal sleeve with internal diameter 0.8 mm made from a needle (BD, Precision Glide, 18 G) is inserted in the hole. The sleeve outside diameter OD=1.3 mm displayed as a black circle in the fingering

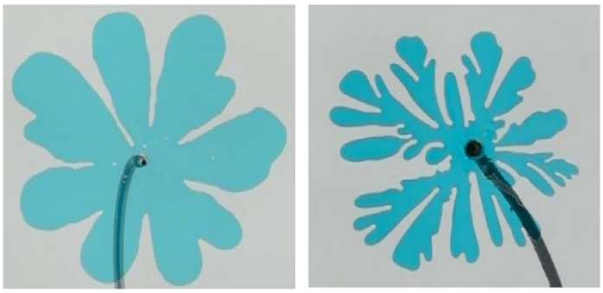

FIG. 2. The classic Saffman-Taylor instability is observed when only one of the required components is used: (a) pure water / oleic acid, (b) 425 mM CPCl solution / silicone oil ($Q = 100$ ml/h, $t = 15$ s).

pattern figures can be used as a reference length scale (with the exception of Fig. 2b with OD=5mm). For injection, a single-syringe infusion pump (Cole-Parmer 74900 series, KDS100) is used, which includes a 60 ml disposable syringe (Luer-Lok tip, BD) connected via plastic tubing to the sleeve on the lower plate. A uniform illumination is provided by a light box (Schott-Fostec), and images are taken from above with a Casio EX-F1 digital camera (color). For better visualization, blue food coloring ($\leq$10%, McCormick) is added to the solution during preparation. Separate tests with no or very little colorant ($\approx 0.2\%$) were performed to show that there is no effect. The final assembly must be done in a matter of seconds, in order to minimize the exposure of liquids before the experiment; multiple trials are made for each condition to ensure consistent results.

An example of the instability in this system is shown in Fig. 1a. The thin, wispy fingers observed when a 400 mM CPCl solution is injected into oleic acid are clearly different than the standard ST instability. To emphasize this difference, we ran experiments with each required component separately: we injected purified water into the Hele-Shaw cell filled with oleic acid (Fig. 2a), and also injected highly concentrated CPCl solution (425 mM) into silicone oil (Fig. 2b). In both cases, typical ST fingering patterns are observed; thus both surfactant solution and the oleic acid are required to produce these unusual patterns. The direct cause of these patterns seems to be a material layer which forms at the interface between the two fluids, best visualized via the darker color of finger's edge in Fig. 1b. These fingers bear a resemblance to some of the chemical gardens produced in a Hele-Shaw cell (see e.g. [17], Figure 3d).

Generally speaking, oleic acid and aqueous solutions do not mix; the material which so strongly affects our hydrodynamic patterns exists only at the interface. However, after many systematic trials we eventually discovered certain ratios of the components (oleic acid, CPCl, water) as well as a preparation protocol which yielded a bulk homogeneous material state [29]. We study the rheological properties of two bulk mixtures: one at about equimolar content of CPCl and oleic acid (13.5 wt% oleic, 11.1 wt% CPCl, 75.4 wt% water), which we refer to here as Gel 1, and one at (15.8, 12.8, 71.4), labelled Gel 2. To prepare these samples, the surfactant is first dissolved in deionized water, and oleic acid is added the next day. This mixture is held at 77°C for a week, stirred a few times per day with a glass rod. The material produced is paste-like and semitransparent. Rheological measurements are performed using a Discovery-HR3 rheometer (TA Instruments) with a cone and plate geometry [29]. The reported values are the average of three trials. A frequency sweep at 1% strain (in the linear regime) for both samples indicate similar behavior, see Fig. 3. We observe the storage modulus G' is about an order of magnitude larger than the loss modulus G'', while both moduli are roughly independent of frequency, a typical behavior for a viscoelastic gel [30], and similar to what was reported for the interfacial rheology of this system [28].

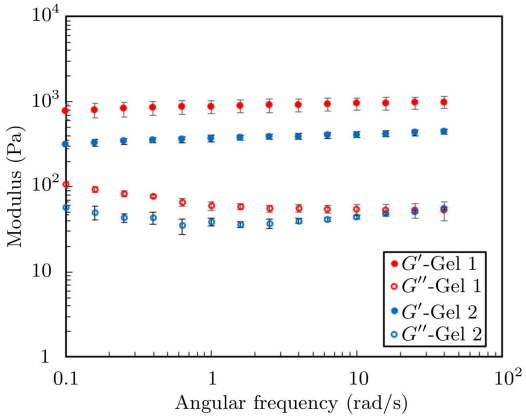

FIG. 3. Viscoelastic behavior of bulk homogeneous surfactant/fatty acid material: Gel 1 (red), and 2 (blue), see text. Closed and open circles show elastic and loss moduli, respectively.

We observe the dynamics of these patterns as the surfactant concentration C or the injection rate Q are varied, the two parameters which should affect the growth rate (thickness) and stretch rate of the material at the interface [7, 21, 28]. Fig. 4 shows various patterns of $C = 50$ mM solution penetrating into oleic acid at different Q. Each frames at time t is chosen based on a criterion Qt =constant, which adjusts for the change in pattern growth rate [31]. The result at high flow rate shows that the fingers are wide, and similar in appearance to the ST instability (Fig. 4d), likely due to the fact that two fluids have less time to react, resulting in a thinner interfacial layer [21, 28] and a slight perturbation to the ST instability.

When the injection rate Q slows down in the classic ST instability, the interface becomes less unstable, and the fingers formed are wider and fewer in number [17, 32].

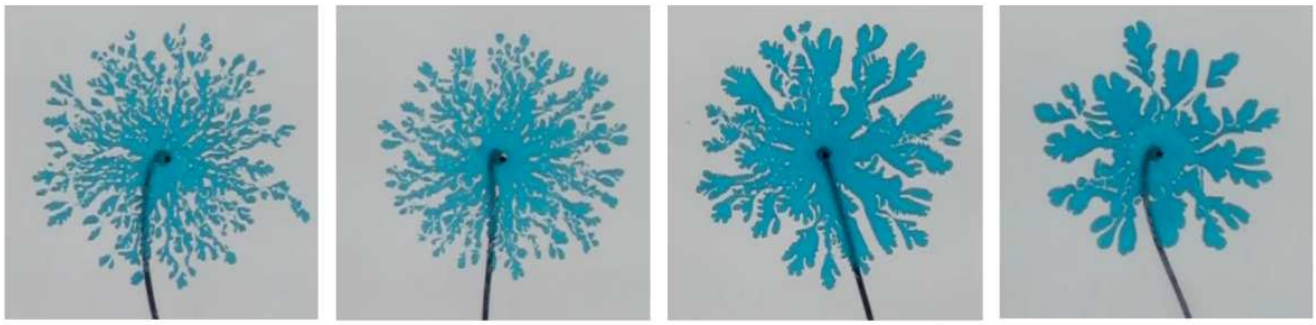

FIG. 4. Fingering pattern made with 50 mM CPCl/oleic acid at time $t = 800/Q$: (a) $Q = 150$ ml/h, (b) $Q = 250$ ml/h, (c) $Q = 350$ ml/h, (d) $Q = 400$ ml/h.

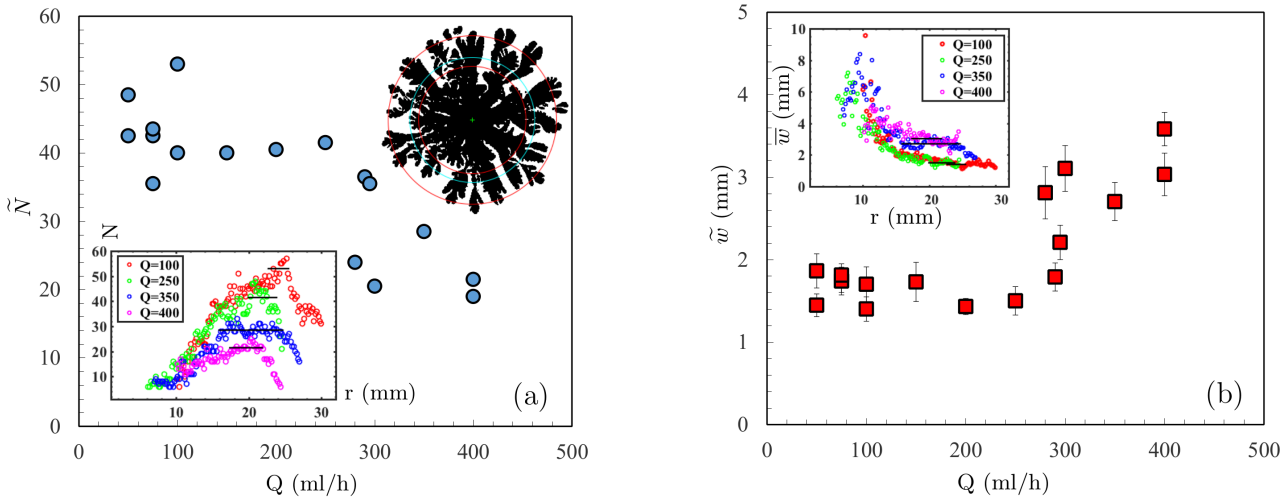

FIG. 5. Quantitative aspects of the finger patterns at 50 mM CPCl, taken at time $t = 800/Q$: (a) the effective number of fingers vs flow rate, (b) the effective width of fingers as a function flow rate. The inset plots show average width and number of fingers measured at varying radii r from the center (see text). The inset pic in (a) shows the binary picture of fingering pattern in Fig. 4c. The blue circle shows the radius where $N = N_{max}$, and the red circles show where N reaches $0.75N_{max}$.

Our observations are remarkably different - reducing the flow rate leads to the formation of *many more* fingers, which are narrower (see Fig. 4, right to left). This may be due to the formation of more gel-like material, as the two components have more time to react, favoring the formation of smaller fingers. This trend is preserved when more data are analyzed, as shown in Fig. 5, where $\widetilde{N}$ and $\widetilde{w}$ represent the effective number of fingers and the effective finger width at time $t = 800/Q$. To obtain these measurements, the color pictures were first converted into binary images in MATLAB. The number of fingers N and average finger width $\overline{w}$ are then measured using the intersection with concentric circles centered on the injection point, as a function of the circle radius r (see inset graphs). The horizontal lines appearing in each inset represent $\widetilde{N}$ or $\widetilde{w}$, and are defined by the interval around N_{max} for which N falls to 75% of N_{max}; $\widetilde{w}$ is then calculated by averaging all $\overline{w}$ in this interval, while $\widetilde{N}$ is the corresponding average of N_{max} and $75\%N_{max}$, i.e. $87.5\%N_{max}$. The error bars shown represent the standard deviation of the measurements averaged, however they do not include other error, such as finger overlap, roundoff in the binary conversion, or pattern asymmetry, which we estimate to be small.

Within the scatter of this data, there is some indication of two regimes, above and below $Q_c \simeq 250$ ml/h. At the slower injection rates $Q < Q_c$, both the number of fingers and average width are roughly constant. However, above Q_c, the finger width begins increasing and the number of fingers decreases. This suggests some sort of yield stress or critical shear rate condition has been reached, possibly related to the strength of the material at the interface [21, 28, 33] or a yield stress effect [34]. Motivated by this opposite dependence of $\widetilde{N}$ and $\widetilde{w}$ on Q, we examined their product, normalized by the circumference of the circle with r_{mean} where the averages were

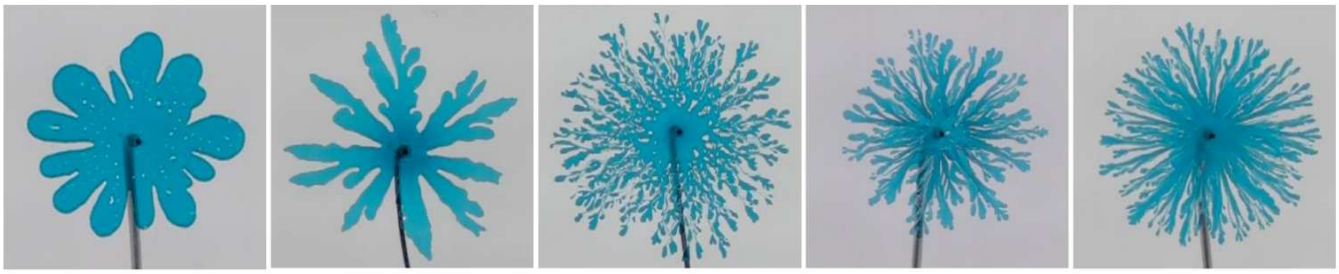

FIG. 6. Fingering pattern made in CPCl/oleic acid at fixed $Q = 100$ ml/h and $t = 8$ s for CPCl concentration of (a) $C = 0.5$ mM, (b) $C = 25$ mM, (c) $C = 50$ mM, (d) $C = 100$ mM, and (e) $C = 200$ mM.

made: $\Gamma = \frac{\widetilde{N}\widetilde{w}}{2\pi r_{mean}}$. This ratio represents the fraction of the circle covered by injected fluid. We find that $\Gamma \simeq 0.5$ is approximately independent of Q, and its value is approximately the same as that measured for an equivalent experiment with pure water and oleic acid [29].

We also studied the dependence on surfactant concentration C (0 to 400 mM), with fixed $Q = 100$ ml/h, as shown in Fig. 6. Even for $C > 0$ but below the critical micelle concentration (CMC $\simeq 1$ mM), we observe a slight but definite change, as the fingers decrease in width and appear to branch less, shown in Fig. 6a. With further increase in C the fingers become dramatically smaller and shorter, sometimes undergoing pinch-off and coalescence processes ($C \simeq 50$ mM), see Fig. 6c. A similar phenomenon has been observed in immiscible two phase systems, where the thermodynamics couples to the flow [35]. For $C \geq 200$ mM, we observe longer and narrower fingers, essentially the same as Fig. 1a. This might be due to the formation of more interfacial material at higher C, resulting in an increased thickness which would impede finger tip-splitting. An increased elasticity of the material with C could also lead to the suppression of tip-splitting, as shown numerically for fingers in a model where the interface is represented as a membrane with both elasticity and surface tension [36].

To quantify the pattern dependence on C, we perform the same analysis for the number $\widetilde{N}$ and width $\widetilde{w}$ of fingers as described above, see Fig. 7. Here $\widetilde{N}$ increases while $\widetilde{w}$ decreases, as C is increased up to 200 mM. Beyond this value, both variables seem to be independent of C. Taking the C and Q dependence together, we conclude that the interfacial material is at "full strength" in the ranges $C \geq 200$ mM and $Q < 250$ ml/h, whereas at either lower concentrations or higher flow rates, the material is either limited by the surfactant supply, stretched too quickly, or not given enough time for formation.

The patterns at the highest concentrations ($C \sim 400$ mM) do not seem to change with Q (100 - 400 ml/h), and appear similar to Fig. 1a. This is in contrast to the low concentration patterns ($C \sim 50$ mM), which become more like the ST instability as Q increases (Fig. 4d). From this we conclude that the reaction has become more rapid at these high concentration, such that the full range of Q are all relatively slow in comparison.

The first question which arises from our observations is: what aspect of oleic acid (absent in silicon oil) is responsible for these unusual patterns and dynamics? As a fatty acid, oleic acid has amphiphilic properties due to a polar carboxylic headgroup and hydrocarbon chain; the physical behavior of fatty acids dispersed in water is directly related to the ionization (deprotonation) state of this carboxylic head, which is influenced by the solution pH [37–41]. Fatty acids remain fully neutral (protonated) in a highly acidic environment, while becoming fully ionized at high pH. In between, both forms (neutral/ionized) exist [38, 42].

We carried out a simple test to check the ionization state of the fatty acid in our system. We mixed 10% by volume of oleic acid with pure water, which resulted in a pH decrease from pH=5.6 to 4.3 in the aqueous phase. Further addition of oleic acid (10% by volume), resulted in a further decrease to pH=4.0. Since each addition moved the solutions towards the more acidic, this suggests that the oleic acid is only partially ionized, and that both neutral and ionized forms exist in our experiments.

It is known that when cationic surfactant molecules

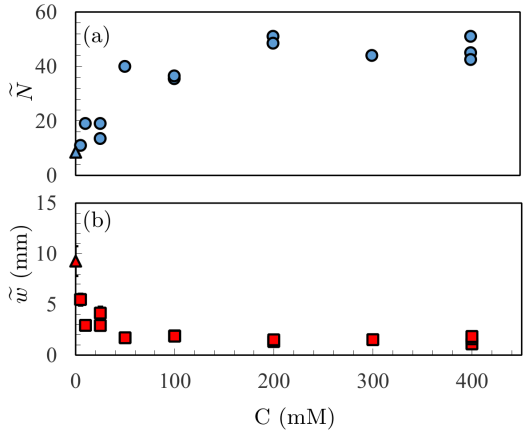

FIG. 7. (a) $\widetilde{N}$, and (b) $\widetilde{w}$ (mm) versus concentration, calculated similar to Fig. 5. Triangle shows C=0, i.e. ST pattern.

FIG. 8. Pattern formed by injecting a 400 mM CPCl solution at Q =100 ml/h into caprylic acid (taken at t=8 s).

are present in fatty acid solution, a wide range of self-assembled structures can form [40, 43]. The molecular organization comes from the fact that ionized fatty acids can associate with the surfactant head cation by electrostatic interactions, similar to what exists in catanionic surfactant systems [41, 44, 45], while neutral and ionized fatty acids interact via hydrogen bonding [40]. There are many studies on different fatty acid/cationic systems [20, 24, 43], other types of carboxylic acid/cationic system (including CPCl) [46, 47], as well as pure catanionic surfactant systems [44, 45]. We expect that the self-assembly of CPCl/oleic acid shares similarities with these systems, although to the best of our knowledge the microstructure, intermolecular interactions, and resultant physical properties have thus far not been studied.

To follow up on this line of reasoning, we used another liquid fatty acid in our Hele-Shaw experiments: caprylic acid - which is 10 times less viscous and half the molecular weight of oleic acid [29]. Using a 400 mM CPCl solution at Q =100 ml/h, we observed a fan-like pattern, as shown in Fig. 8. Note that the two liquids in this experiment are close in viscosity [28], while the fan-shaped fingers are quite similar to what has been observed with a micellar material between two aqueous solutions ([21], Fig. 5). Although at lower C we observed essentially the ST instability, this experiment supports the hypothesis that the carboxylic head is responsible for the formation of interfacial material. Additional experiments with a low viscosity oil without carboxylic head (tetradecane) showed no evidence of material forming at the interface.

We have studied the patterns formed in a Hele-Shaw cell when a cationic surfactant solution is injected into two fatty acids, and studied the effects of the material forming at the interface on these patterns. At low surfactant concentrations, the patterns show fewer, wider fingers with increasing injection rate Q. At fixed Q, narrower fingers of increasing number are seen with increasing concentration (up to C=200 mM). At the highest concentrations, thin tendril structures are seen in oleic acid, and a fan-like instability is seen with caprylic acid. Dynamic rheology on certain homogeneous bulk samples of oleic acid/CPCl/water indicate that this surfactant/fatty acid material is a gel, although these mixtures may or may not be similar to the interfacial material formed during flow.

Given the original connection between the work of Saffman & Taylor and oil recovery in porous media [1], it is interesting that our results may have relevance to aspects of crude oil processing, such as the formation of gel-like structures when a crude oil component (tetrameric acid) with a carboxylic head group reacts with calcium ions at a water surface [24, 48]. We expect that further study of the dynamics of this surfactant/fatty acid material and its formation at fluid interfaces may also have implications for related phenomena in drug delivery [49] and the production of artificial cells [42, 50, 51].

We would like to thank R. Colby and R. Geist, F. Haudin, and A. De Wit for experimental assistance/advice, and L. Ibarra Bracamontes, Y. Nagatsu, D. Takagi, L. Zarzar, and R. Hickey for helpful discussions. This work was supported by NSF Grant DMS-1217277.

* Also at: ImmunoDynamics Group, Center for Cancer Research, National Cancer Institute, National Institutes of Health, Bethesda, MD.

[1] P. G. Saffman and G. I. Taylor, Proc. Roy. Soc. Lond. **245**, 312–329 (1958) .
[2] G. M. Homsy, Ann. Rev. Fluid Mech. **19**, 271–311 (1987).
[3] J. Nittmann, G. Daccord, and H. E. Stanley, Nature **314**, 141-144 (1985).
[4] J. Nittmann, Physica A **140**, 124-133 (1986).
[5] G. Daccord, J. Nittmann, and H. E. Stanley, Phys. Rev. Lett. **56**, 336 (1986).
[6] H. Zhao, and J. V. Maher, Phys. Rev. E **47**, 4278 (1993).
[7] L. Kondic, M. J. Shelley, and P. Palffy-Muhoray, Phys. Rev. Lett. **80**, 1433 (1998).
[8] H. Van Damme, F. Obrecht, P. Levitz, L. Gatineau, C. Laroche, Nature **320**, 731–733 (1986).
[9] E. Lemaire, P. Levitz, G. Daccord, and H. Van Damme, Phys. Rev. Lett. **67**, 2009-2012 (1991).
[10] S. S. Park and D. J. Durian, Phys. Rev. Lett. **72**, 3347 (1994).
[11] A. De Wit and G. M. Homsy, J. Chem. Phys. **110**, 8663 (1999).
[12] J. Fernandez, G. M. Homsy, J. Fluid Mech. **480**, 267 (2003).
[13] Y. Nagatsu, K. Matsuda, Y. Kato, and Y. Tada, J. Fluid Mech. **571**, 475-493 (2007).
[14] Y. Nagatsu, C. Iguchi, K. Matsuda, Y. Kato, and Y. Tada, Phys. Fluids **22**, 024101 (2010).
[15] F. Haudin, J. H. E. Cartwright, F. Brau, A. De Wit, PNAS **111**, 17363–17367 (2014).
[16] Y. Nagatsu, Y. Ishii, Y. Tada, and A. De Wit, Phys. Rev. Lett. **113**, 024502 (2014).
[17] F. Haudin, and A. De Wit, Phys. Fluids **27**, 113101

(2015).
[18] F. Haudin, V. Brasiliense, J. H. Cartwright, F. Brau, and A. De Wit, Phys. Chem. Chem. Phys. **17**, 12804-12811 (2015).
[19] Y. Nagatsu, A. Hayashi, M. Ban, Y. Kato, Y. Tada, Phys. Rev. E **78**, 026307 (2008).
[20] Y. Sumino, H. Kitahata, Y. Shinohara, N. L. Yamada, and H. Seto, Langmuir **28**, 3378-3384 (2012).
[21] T. Podgorski, M. C. Sostarecz, S. Zorman, A. Belmonte, Phys. Rev. E **76**, 016202 (2007).
[22] J. Cardiel, D. Takagi, H-F. Tsai, and A. Q. Shen, Soft Matter **12**, 8226–8234 (2016).
[23] A. R. White and T. Ward, Chaos **22**, 037114 (2012).
[24] S. Simon, S. Subramanian, B. Gao, and J. Sjöblom, Ind. Eng. Chem. Res.**54**, 8713–8722 (2015).
[25] J. P. Rane, V. Pauchard, A. Couzis, and S. Banerjee, Langmuir **29**, 4750–4759 (2013).
[26] V. Pauchard, J. P. Rane, and S. Banerjee, Langmuir **30**, 12795 (2014).
[27] A. Jimenez, S. Lecuyer, H. A. Stone, A. Belmonte, Bull. Am. Phys. Soc. **52**, JC.00001 (2007).
[28] Z. Niroobakhsh, A. Belmonte, submitted to J. Non-Newtonian Fluid Mech.
[29] Z. Niroobakhsh, A. Belmonte, in preparation.
[30] H. A. Barnes, J. F. Hutton, and K. Walters, *An Introduction to Rheology* (Elsevier, Amsterdam, 1989).
[31] I. Bischofberger, R. Ramachandran, and S. R. Nagel, Nature Comm. **5**, 5265 (2014).
[32] C. T. Tan and G. M. Homsy, Phys. Fluids **29**, 3549 (1986).
[33] J. R. Gladden and A. Belmonte, Phys. Rev. Lett. **98**, 224501 (2007).
[34] A. Lindner, P. Coussot, and D. Bonn, Phys. Rev. Lett. **85**, 314–317 (2000).
[35] X. Fu, L. Cueto-Felgueroso, and R. Juanes, Phys. Rev. E **94**, 033111 (2016).
[36] M. Zhao, A. Belmonte, S. Li, X. Li, and J. Lowengrub, J. Comp. Appl. Math. **307**, 394–407 (2016).
[37] D. M. Small, J. Amer. Oil Chem. Soc. **45**, 108–119 (1968).
[38] D. P. Cistola, J. A. Hamilton, D. Jackson, and D. M. Small, Biochemistry **27**, 1881-1888 (1988).
[39] S. Salentinig, L. Sagalowicz, and O. Glatter, Langmuir **26**, 11670-11679 (2010).
[40] A. L. Fameau, and T. Zemb, Adv. Colloid Interface Sci. **207**, 43–64 (2014).
[41] D. Vila-Vicosa, V. H. Teixeira, A. M. Baptista, and M. Machuqueiro, J. Chem. Theory Comp. **11**, 2367–2376 (2015).
[42] A. J. Markvoort, N. Pfleger, R. Staffhorst, P. A. J. Hilbers, R. A. Van Santen, J. Antoinette Killian, and B. De Kruijff. Biophys. J. **99**, 1520–1528 (2010).
[43] C. Noirjean, F. Testard, J. Jestin, O. Tache, C. Dejugnat, and D. Carriere, Soft Matter **10**, 5928–5935 (2014).
[44] E. W. Kaler, A. K. Murthy, B. E. Rodriguez, and J. A. Zasadzinski, Science **245**, 1371-1375 (1989).
[45] L. Chiappisi, H. Yalcinkaya, V. K. Gopalakrishnan, M. Gradzielski, and T. Zemb, Colloid and Polymer Sci. **293**, 3131-3143 (2015).
[46] J. Linet Rose, B. V. R. Tata, V. K. Aswal, P. A. Hassan, Y. Talmon, and L. Sreejith, European Phys. J. E **38**, 1–9 (2015).
[47] Z. Liu, P. Wang, S. Pei, B. Liu, X. Sun, and J. Zhang, Colloids and Surfaces A **506**, 276–283 (2016).
[48] B. Brocart, M. Bourrel, C. Hurtevent, J. L. Volle, and B. Escoffier, J. Dispersion Sci. Tech. **28**, 331–337 (2007).
[49] K. Patel, V. Sarma, and P. Vavia, DARU J. Pharmaceutical Sci. **21**, 1 (2013).
[50] M. Hanczyc, S. M. Fujikawa, and J. W. Szostak, Science **302**, 618–622 (2003).
[51] K. Morigaki and P. Walde, Curr. Opin. Colloid Interface Sci. **12**, 75–80 (2007).